Chiral Nanoparticles

Intense Optical Activity from Three-Dimensional Chiral Ordering of Plasmonic Nanoantennas**

Andrés Guerrero-Martínez, Baptiste Auguié, José Lorenzo Alonso-Gómez, Zoran Džolić, Sergio Gómez-Graña, Mladen Žinić, M. Magdalena Cid,* and Luis M. Liz-Marzán**

Noble-metal nanoparticles[1] with localized surface-plasmon resonances (LSPR) have been recently used to prepare new materials with improved optical circular dichroism.[2] This interest stems from a wide range of applications in biology and physics, including the structural determination of proteins and DNA[3] and the pursuit of negative refraction.[4] Surface-plasmon-mediated circular dichroism (SP-CD) in solution has been explored to date using small spherical metal particles, invariably resulting in moderate signals over a narrow spectral range.[5–10] In contrast, we present herein a novel class of metamaterial consisting of gold nanorods (NRs) organized in three-dimensional (3D) chiral structures and yielding a record circular dichroism anisotropy factor for metal nanoparticles (> 0.02) across visible and near-infrared (Vis–NIR) wavelengths (600–900 nm). The fabrication process can be easily upscaled, as it involves the self-assembly of gold nanorods on a fiber backbone with chiral morphology. Our measurements are fully supported by theoretical modeling based on coupled dipoles, unraveling the key role of gold nanorods in the chiroptical response.

Three major strategies have been considered for the generation of SP-CD responses: synthesis of metal clusters with an intrinsically chiral surface,[11,12] adsorption of chiral molecules onto achiral metal nanoparticles,[5,13] and organization of nanoparticles into three-dimensional chiral arrangements.[5–10] Herein, we present a record level of optical activity with a chiral assembly of NRs, which we interpret as SP-CD. Known as plasmonic nanoantennas,[14] these particles are characterized by the resonant collective interaction of their conduction electrons with light in the form of both scattering and absorption, with resonance frequencies that can be tuned across the Vis–NIR spectrum by simply changing the aspect ratio of the nanocrystals.[15] Moreover, the LSPR of NRs is very sensitive to the presence and relative orientation of neighboring particles.[16] These two properties combined make NRs promising building blocks for intense and tunable SP-CD. We have designed a new nanocomposite using a self-assembly strategy[17] with NRs adsorbed onto a scaffold of supramolecular fibers with chiral morphology through specific non-covalent interactions.

NRs with an average length of 45 nm and average width of 17 nm were prepared by a seeding growth method,[18] and subsequently coated with the amphiphilic polymer poly(vinylpyrrolidone) (PVP) in ethanol.[19] Fibers having a chiral morphology were obtained by adding water to a DMF/ethanol solution of anthraquinone-based oxalamide **1** (Figure 1a),[20] forming a fluid dispersion (see the Supporting Information for experimental details). In Figure 1b,c, we present scanning electron microscopy (SEM) images of twisted fibers with right- (*P*) and left-handedness (*M*), corresponding to (*R*)-**1** and (*S*)-**1**, respectively, with widths in the hundred-nanometer range and lengths of several micrometers.

For the preparation of the nanocomposites, a solution of NRs was added to either the *P* or *M* fiber dispersion, leading to a spontaneous assembly of nanoparticles onto the fiber surface (Figure 1d,e). NRs are preferentially aligned along the longitudinal direction of the fibers through non-covalent interactions. The UV/Vis absorbance spectra of the nanocomposites in solution reveal the characteristic resonance bands associated with the transverse (ca. 520 nm) and longitudinal (ca. 720 nm) LSPR modes of NRs (Figure 2b). Furthermore, the UV/Vis spectra also feature the background contribution from the supramolecular fibers (at ca. 400 nm). The CD spectra of the nanocomposites consistently present a strong bisignated Cotton effect[21] at the position of the longitudinal LSPR (Figure 2a). Both enantiomeric nanocomposites show mirror-image CD responses, allowing us to disregard artifacts originating from linear dichroism and/or linear birefringence (see the Supporting Information),[22] which may occur in samples with macroscopic anisotropy.[21] For comparison, we also prepared *P* and *M* nanocomposites

[*] Dr. A. Guerrero-Martínez, Dr. B. Auguié, S. Gómez-Graña,
Prof. L. M. Liz-Marzán
Departamento de Quimica Fisica and Unidad Asociada CSIC
Universidade de Vigo
36310 Vigo (Spain)
Fax: (+34) 986-812-556
E-mail: lmarzan@uvigo.es

Dr. J. L. Alonso-Gómez, Prof. M. M. Cid
Departamento de Quimica Orgánica, Universidade de Vigo
36310 Vigo (Spain)
E-mail: mcid@uvigo.es

Dr. Z. Džolić, Prof. M. Žinić
Laboratory of Supramolecular and Nucleoside Chemistry
Division of Organic Chemistry and Biochemistry
Rudjer Boskovic Institute, 10002 Zagreb (Croatia)
E-mail: mladen.zinic@irb.hr

Supporting information for this article is available on the WWW under http://dx.doi.org/10.1002/anie.201007536.
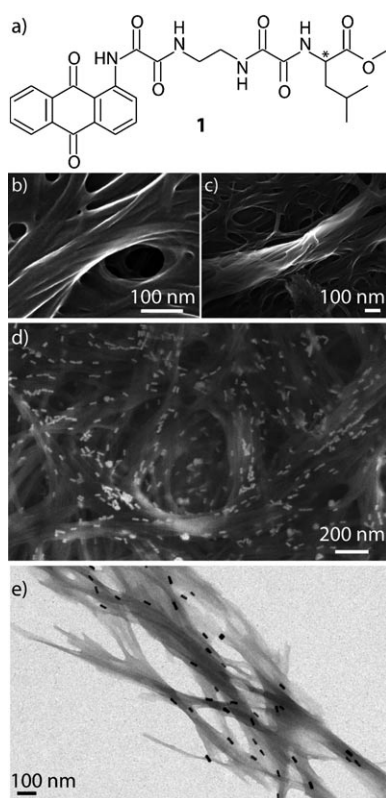
Figure 1. Representative electron micrographs of the anthraquinone-based oxalamide fibers with chiral morphology and nanocomposites. a) Chemical structure of the anthraquinone-based oxalamide **1**, showing the asymmetric carbon atom. b,c) Scanning electron microscopy (SEM) graphs of the *P* and *M* fibers, respectively, after solvent evaporation. d) SEM micrograph of the *P* bulk nanocomposite. e) Transmission electron microscopy (TEM) image of the *M* nanocomposite showing twisted fibers with adsorbed nanorods.

Figure 2. a) Experimental CD and b) UV/Vis spectra in fluid suspensions (0.1 cm path length). Solid lines show the results for gold NRs (length 45 nm, width 17 nm); dashed lines show the results for gold nanospheres (average diameter 15 nm). CD spectra are shown for both *P* (red) and *M* nanocomposites (blue). Both enantiomeric nanocomposites show identical UV/Vis response (only the *P* nanocomposite spectrum is shown). The concentration of gold NRs and nanospheres in the nanocomposite solutions were 1.7×10^{-9} mol L^{-1} and 6.3×10^{-9} mol L^{-1}, respectively.

with gold nanospheres[23] (average diameter 15 nm) and measured their UV/Vis and CD spectra (Figure 2a,b). No optical activity was observed at the LSPR wavelength (ca. 520 nm) for gold nanospheres. This result suggested that plasmon-induced CD mechanisms arising from the interaction between fibers and nanoparticles are not significant under our experimental conditions.[13]

We propose that the observed SP-CD signal originates from a 3D chiral arrangement of the NRs. Working with this hypothesis, we now set out to explain our results with a coupled-dipole model,[24,25] in which each particle is described as an electric dipole. In this framework, Govorov and co-workers recently predicted the possibility of inducing SP-CD in helical arrangements of gold nanospheres.[26] Nevertheless, they concluded that small variations of geometry or composition in the system can greatly diminish the CD signal (Figure 3a). Accordingly, a sample with a finite amount of disorder is expected to show only negligible SP-CD. This was confirmed by our experimental findings for gold nanospheres (Figure 2a).

In contrast, we predict a robust SP-CD for a chiral structure bearing elongated particles that are oriented along a helix (Figure 3b; the model is fully described in the Supporting Information). Notably, a chiral arrangement of nano-
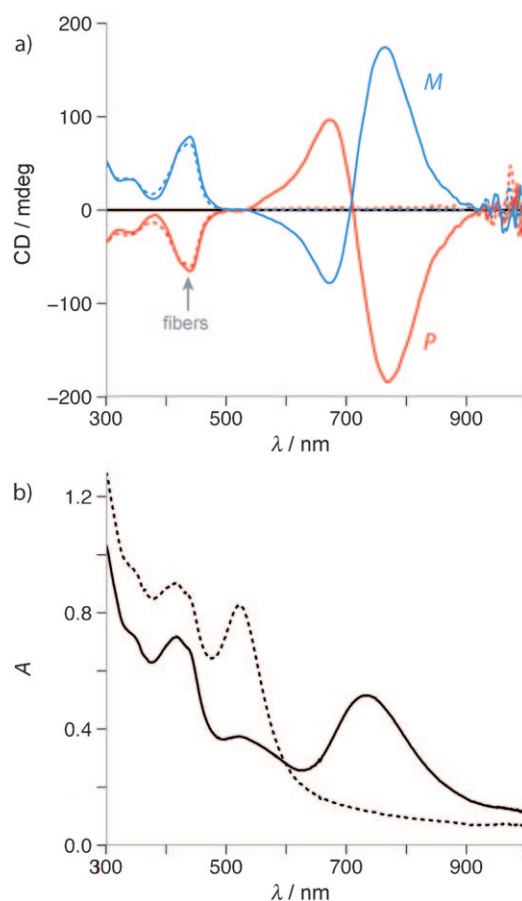
particles requires at least four nanospheres but only two NRs. Furthermore, the intensity of the normalized SP-CD rapidly increases with the number of NRs in the assembly. Surprisingly, even a slight departure from sphericity (aspect ratio 1:1.1) is sufficient to greatly improve the robustness of the CD lineshape with respect to the number of the particles present in the system.

A model for our real system that mimics the nanocomposite morphology is shown in Figure 4a. NRs immersed in a homogeneous medium were positioned on a 100 nm radius tube, and each nanoparticle was oriented following a helix with a 3 micrometer pitch. To limit the number of free variables in the model, we considered the simplest configuration of two NRs (Figure 4b), thereby restricting the model to one-to-one interactions between particles. CD spectra for a monodisperse sample were simulated by varying the relative position of the two particles independently along z and β (details on the numerical procedure are provided in the Supporting Information). Summation of all spectra provides
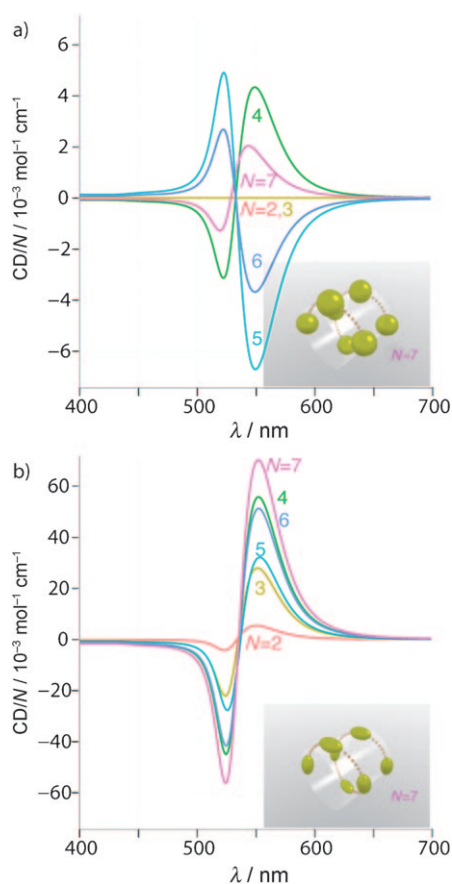
Figure 3. Simulated CD spectra using a coupled-dipole model. Nanoparticles immersed in a homogeneous medium of refractive index 1.33 are arranged following a helical curve with 12 nm radius and 15 nm pitch. The nanoparticles are placed every 90 degrees of gyration on the helix. The simulated spectra are scaled by the number of particles N ($N = 2$–7). a) Spheres with 5 nm radius, reproducing the results of Govorov and co-workers.[26] b) Prolate ellipsoids of semi-axes 4.5 nm × 5 nm (aspect ratio 1:1.1) with the major axis tangential to the helix.

Figure 4. Representation of the nanocomposite and corresponding calculated CD spectra. a) General sketch of the system. NRs are randomly positioned onto the surface of a cylinder of radius $R = 100$ nm. The orientation of each particle is defined so that its long axis is tangential to a helical curve of 3 μm pitch. b) Same as in (a), but with only two particles. The parameters describing the relative position of the two NRs are the distance z along the cylinder axis and the rotation angle β around the cylinder. c) Modeled CD and d) extinction spectra ε using the coupled-dipole model described in the Supporting Information. The calculations are presented for monodisperse (red) and polydisperse (black) particle size distributions. In (d), the dashed curves represent the average extinction spectra without electromagnetic coupling between dipoles (experimentally, this corresponds to a dilute solution of nanoparticles), showing no significant differences in the LSPR. e) Experimental CD and f) extinction spectra of the *P* nanocomposite reproduced from Figure 2.

the overall CD spectrum (Figure 4c), which predicts a bisignated Cotton effect with a more intense low-energy wing and a zero-crossing point slightly blue-shifted from the longitudinal LSPR. The bisignated lineshape, which is well reproduced with this minimal two-rod model, is strongly reminiscent of the characteristic response of molecules with coupling between two identical chromophores (exciton coupling theory).[27] This analogy is not fortuitous, as both models are based on dipole–dipole interactions, albeit at a different scale. The major difference between experimental and modeling results was found in the width of the CD features. Polydispersity was therefore introduced in the model using the distribution of particle sizes obtained from TEM measurements (see the Supporting Information). This resulted in an inhomogeneous broadening of the LSPR and the SP-CD (Figure 4c,d). With this addition our model faithfully reproduced the experimental CD spectra (Figure 4e,f). The discrepancy in absolute SP-CD intensity can be explained by different factors. The model ignores interactions between more than two particles. Additionally, interactions between
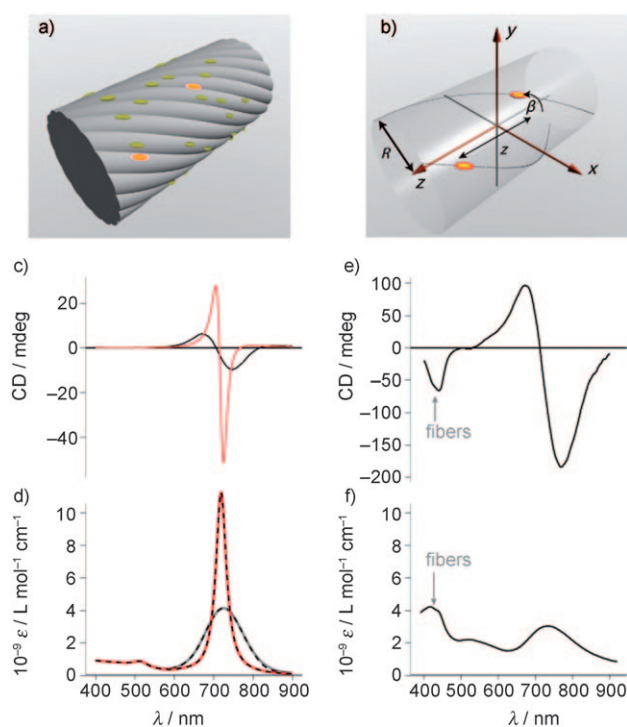
particles in direct contact cannot be considered within the coupled-dipole approximation.[11,25]

The optical activity of chiral systems is often measured through the anisotropy factor (*g*-factor) [Equation (1)]:[28]

$$g = \frac{\Delta\varepsilon}{\varepsilon} \tag{1}$$

where $\Delta\varepsilon$ and ε are the molar circular dichroism and molar extinction, respectively. Figure 5a shows the concomitant increase in the *g*-factor with the concentration of NRs in the nanocomposite, reaching a maximum value of 0.022. At a low concentration of particles, TEM images show partial coverage of NRs adsorbed on the surface of the fibers, corresponding to relatively large interparticle distances and, consequently, to weak electromagnetic coupling and moderate SP-CD. Upon increasing the concentration of NRs, the coverage extends until complete saturation of the fiber surface, yielding the most intense CD and the maximum *g*-factor.
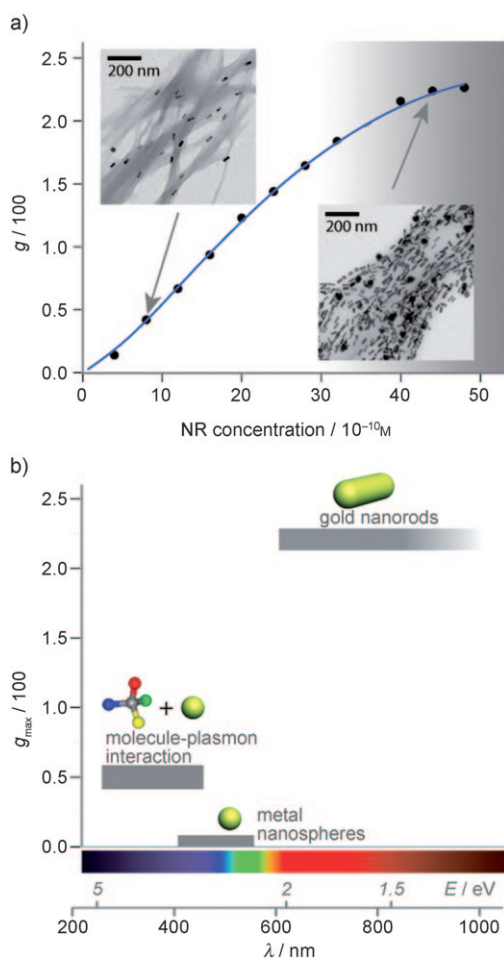
Communications

Figure 5. Anisotropy factor (g-factor) of the nanocomposite and comparison with other chiral nanoparticle systems. a) Evolution of the g-factor with the concentration of NRs, maintaining constant the concentration of P fibers in the nanocomposite. The g-factor reaches a maximum value of 0.022 upon saturation of the fiber surface with particles (TEM insets). b) Representative values of chiroptical metal nanoparticles in fluid media with strong anisotropy factors and the corresponding typical spectral ranges.

As a comparison with other relevant chiroptical metal nanoparticles in solution, Figure 5b shows representative values of the highest reported g-factors and their corresponding spectral ranges. In the UV region, the g-factor of organic molecules can be enhanced by small metal nanospheres up to 0.005.[13] Additionally, small metal nanospheres with SP-CD only register values below 0.001.[5–10] In the present study, we obtained outstanding SP-CDs from NRs in fluid suspensions with g-factors as high as 0.022 covering a wide Vis–NIR range.[29] This value is comparable with the highest g-factors reported for molecules such as polyaromatic compounds (0.05),[30] alleno–acetylenic macrocycles (0.01),[31] and protein complexes (0.06).[32] The potential of localized plasmons in generating strong SP-CD signal is expected to be most fully realized for nanostructures with sizes in the hundred-nanometer range (such as a dimer of NRs presented herein), where the dimensions are commensurate with the intrinsic helicity of incident light.

The original combination of NRs with a 3D chiral structure proposed herein paves the way for a new realm of applications for circular dichroism. We experimentally demonstrated unprecedented levels of anisotropy factor in the visible–near infrared region using a versatile and generic self-assembly strategy. We thus anticipate the use of such plasmonic nanoantennas as powerful chirality probes upon attachment to proteins or DNA for in situ structure determination,[33,34] by selecting the appropriate dimensions, morphology, and functionalization of the metal nanoparticles. Other particularly promising applications for this new class of chiroptical metamaterials include non-linear optics,[35] negative refraction,[4] and surface-enhanced Raman optical activity.[36] We are currently focusing our effort on the non-trivial task of preparing new organic precursors to obtain chiral fibers in which the helix morphology is better defined, and parameters such as diameter and pitch are controlled, with the aim of obtaining metal nanoparticle composites with further enhanced optical activity.

[1] S. Maier, *Plasmonics: Fundamentals and Applications*, Springer, Heidelberg, **2007**.
[2] D. B. Amabilino, *Chirality at the Nanoscale*, Wiley-VCH, Weinheim, **2009**.
[3] R. Quidant, M. Kreuzer, *Nat. Nanotechnol.* **2010**, *5*, 762–763.
[4] J. B. Pendry, *Science* **2004**, *306*, 1353–1355.
[5] G. Shemer, O. Krichevski, G. Markovich, T. Molotsky, I. Lubitz, A. B. Kotlyar, *J. Am. Chem. Soc.* **2006**, *128*, 11006–11007.
[6] J. George, K. G. Thomas, *J. Am. Chem. Soc.* **2010**, *132*, 2502–2503.
[7] W. Chen, A. Bian, A. Agarwal, L. Liu, H. Shen, L. Wang, C. Xu, N. A. Kotov, *Nano Lett.* **2009**, *9*, 2153–2159.
[8] A. J. Mastroianni, S. A. Claridge, A. P. Alivisatos, *J. Am. Chem. Soc.* **2009**, *131*, 8455–8459.
[9] I. Lieberman, G. Shemer, T. Fried, E. M. Kosower, G. Markovich, *Angew. Chem.* **2008**, *120*, 4933–4935; *Angew. Chem. Int. Ed.* **2008**, *47*, 4855–4857.
[10] T. Molotsky, T. Tamarin, A. B. Moshe, G. Markovich, A. B. Kotlyar, *J. Phys. Chem. C* **2010**, *114*, 15951–15954.
[11] C. Gautier, T. Bürgi, *J. Am. Chem. Soc.* **2006**, *128*, 11079–11087.
[12] C. Gautier, T. Bürgi, *ChemPhysChem* **2009**, *10*, 483–492.
[13] A. O. Govorov, Z. Fan, P. Hernandez, J. M. Slocik, R. R. Naik, *Nano Lett.* **2010**, *10*, 1374–1382.
[14] L. Novotny, B. Hecht, *Principles of nano-optics*, Cambridge University Press, Cambridge, **2006**.
[15] J. Pérez Juste, I. Pastoriza Santos, L. M. Liz-Marzán, P. Mulvaney, *Coord. Chem. Rev.* **2005**, *249*, 1870–1901.
[16] A. M. Funston, C. Novo, T. J. Davis, P. Mulvaney, *Nano Lett.* **2009**, *9*, 1651–1658.
[17] G. M. Whitesides, B. Grzybowski, *Science* **2002**, *295*, 2418–2421.
[18] N. R. Jana, L. Gearheart, S. O. Obare, C. J. Murphy, *Langmuir* **2002**, *18*, 922–927.
[19] C. Graf, D. L. J. Vossen, A. Imhof, A. van Blaaderen, *Langmuir* **2003**, *19*, 6693–6700.
[20] Z. Džolić, M. Cametti, A. Dalla Cort, L. Mandolini, M. Žinić, *Chem. Commun.* **2007**, 3535–3537.

[21] N. Berova, K. Nakanishi, R. W. Woody, *Circular Dichroism: Principles and Applications*, Wiley, New York, **2000**.

[22] L. D. Barron, *Molecular Light Scattering and Optical Activity*, Cambridge University Press, Cambridge, **2004**.

[23] J. Turkevich, P. C. Stevenson, J. Hillier, *Discuss. Faraday Soc.* **1951**, *11*, 55 – 75.

[24] K. L. Kelly, A. A. Lazarides, G. C. Schatz, *Comput. Sci. Eng.* **2001**, *3*, 67 – 73.

[25] B. T. Draine, P. J. Flatau, *J. Opt. Soc. Am. A* **1994**, *11*, 1491 – 1499.

[26] Z. Fan, A. O. Govorov, *Nano Lett.* **2010**, *10*, 2580 – 2587.

[27] N. Harada, K. Nakanishi, *Circular Dichroic Spectroscopy— Exciton Coupling in Organic Stereochemistry*, Oxford University Press, Oxford, **1983**.

[28] N. Berova, L. D. Bari, G. Pescitelli, *Chem. Soc. Rev.* **2007**, *36*, 914 – 931.

[29] High optical activities have been reported in the case of metal nanoparticles in non-fluid media, such as gels and films, where linear dichroism and birefringence artifacts cannot be disre-

garded; see: a) Y. Li, M. Liu, *Chem. Commun.* **2008**, 5571 – 5573; b) H. S. Oh, S. Liu, H. Jee, A. Baev, M. T. Swihart, P. N. Prasad, *J. Am. Chem. Soc.* **2010**, *132*, 17346 – 17348.

[30] R. S. Walters, C. M. Kraml, N. Byrne, D. M. Ho, Q. Qin, F. J. Coughlin, S. Bernhard, R. A. J. Pascal, *J. Am. Chem. Soc.* **2008**, *130*, 16435 – 16441.

[31] J. L. Alonso-Gómez, P. Rivera-Fuentes, N. Harada, N. Berova, F. Diederich, *Angew. Chem.* **2009**, *121*, 5653 – 5656; *Angew. Chem. Int. Ed.* **2009**, *48*, 5545 – 5548.

[32] R. M. Pearlstein, R. C. Davis, S. L. Ditson, *Proc. Natl. Acad. Sci. USA* **1982**, *79*, 400 – 402.

[33] M. J. García-Parajo, *Nat. Photonics* **2008**, *2*, 201 – 203.

[34] E. Hendry, T. Carpy, J. Johnston, M. Popland, R. V. Mikhaylov-skiy, A. J. Lapthorn, S. M. Kelli, L. D. Barron, N. Gadegaard, M. Kadodwala, *Nat. Nanotechnol.* **2010**, *5*, 783 – 787.

[35] U. Gubler, C. Bosshard, *Nat. Mater.* **2002**, *1*, 209 – 210.

[36] C. Johannessen, S. Abdali, *Spectroscopy* **2007**, *21*, 143 – 149.